JOURNAL OF SOLID STATE CHEMISTRY 94, 185–196 (1991)

The Use of Acetates as Precursors for the Low-Temperature Synthesis of $LiMn_2O_4$ and $LiCoO_2$ Intercalation Compounds

P. BARBOUX,* J. M. TARASCON, AND F. K. SHOKOOHI

*Bellcore, Red Bank, New Jersey 07701; and *CNRS, Université Pierre et Marie Curie, Paris, France*

Received March 25, 1991; in revised form May 23, 1991

The spinel $LiMn_2O_4$ and layered $LiMO_2$ (M = Co, Ni) compounds, which are of potential interest for Li intercalation applications, have been synthesized at low temperatures from aqueous solutions of hydroxides, nitrate, and acetate salts. These phases can be prepared in bulk or thick-film form with their crystallization temperature being strongly dependent on oxygen pressure, annealing time, and Li/transition-metal (M) ratio. For instance, we succeeded in preparing the spinel $Li_xMn_2O_4$ (x = 1) at temperatures as low as 300°C, whereas a temperature of 500°C was needed to obtain the $LiCoO_2$ phase. Rechargeable Li batteries using the $LiMn_2O_4$ powders, synthesized at low temperatures, show good capacity and good cycling behavior. Larger amounts of Li ($x > 1$) cannot be directly introduced into the spinel phase by heat treatment under less oxidizing atmospheres obtained by use of mixtures of argon and oxygen.

Introduction

It is unlikely that room-temperature secondary Li batteries will reach the marketplace because of safety and rechargeability problems associated with the use of Li metal as the negative electrode. To alleviate these problems several authors have proposed the concept of a "rocking-chair" battery (*1–4*) (i.e., a battery that uses, instead of free Li metal, an intercalation compound as the negative electrode). Recently, two battery companies (*5–6*) have demonstrated that this concept could work by announcing the commercialization of rocking-chair cells based on $LiCoO_2$/electrolyte/C and $LiNiO_2$/electrolyte/C, respectively. Since it appears that the next generation of Li-based secondary batteries will be based on the rocking-chair concept, the chemistry of the Li-based intercalation compounds $LiMn_2O_4$ and $LiMO_2$ (M = Co, Ni) has stimulated a great deal of interest.

For application considerations it is important to determine the lowest temperature at which a phase can be synthesized without affecting its electrochemical properties. These properties are usually very sensitive to their preparation route as well as to the morphology and grain size of the resulting powders. As an example, secondary Li cells containing electrochemically deposited γ-MnO_2 (EMD) as the positive electrode cycle poorly, whereas cells using a cathode prepared by heating the EMD in the presence of LiOH at 400°C cycle better (*7, 8*). Concerning grain size, it has been shown in recent electrochemical studies of cells using $LiMn_2O_4$ as the positive electrode (*9*) that cell reversibility, polarization, and capacity

0022-4596/91 $3.00

were greatly improved when cathode powders having the smallest particle size were used.

Solution techniques (because of homogeneous mixing of the starting components) have always been used, rather than solid state reactions, to lower the synthesis temperature of a compound and to obtain powders with smaller grain size. Furthermore, lowering the synthesis temperature could be a way to improve the morphology of the powders. We report herein the low temperature (<400°C) synthesis of $LiMn_2O_4$ and $Li(Co/Ni)O_2$ phases by means of a new solution process.

The solution technique known as sol-gel processing consists of the condensation of metal oxide networks from solution precursors. In the case of Mn, this can be achieved through hydrolysis of Mn(II) salts in aqueous solution in the presence of a stabilizing agent such as gelatin (*10*) or through the reduction of Mn(VII) salts (*11, 12*). We have used the first method by investigating the hydrolysis of acetate and nitrate solutions of Mn, Ni, and Co. This hydrolysis was promoted by the addition of solutions of Li and ammonium hydroxides. We found that this method could produce a gel-like solid that could be used to prepare both bulk and thick-film samples whose electrochemical behavior will also be presented in this paper.

Experimental

Manganous nitrate (0.8 *M*) or acetates of Mn (0.8 *M*), Ni (0.5 *M*), and Co (0.3 *M*) were used for preparing the starting aqueous solutions. LiOH (1 *M*) in the appropriate ratio with the metal was mixed with an amount of NH_4OH (3 *M*) necessary to supply 2 OH ions per metal. The mixed hydroxide solutions were quickly added to the metal salt solution with violent stirring. Gelatinous precipitates were instantaneously obtained. We mean by gelatinous precipitate a macroscopically homogeneous and viscous phase composed of solid particles of metal hydroxide dispersed in the aqueous solvent. Since lithium and ammonium salts are very soluble, these cations probably remain localized in the liquid phase or some may be absorbed at the surface of the particles. The gelatinous precipitates remained stable and homogeneous for hours (Mn), days (Ni), and weeks (Co). However, the solution containing manganese had to be protected from oxygen ambient in order to avoid the formation of Mn(III) containing precipitates at this pH (pH 7 to 8). Afterward, a separation is observed between a colorless supernatant liquid (very slightly colored for Co due to traces of amine complex) and a true precipitate. This relative instability can be attributed to the presence of Li^+ ions that cause flocculation of the solid particles.

If, before their flocculation, the gelatinous slurries are dried at up to 150°C they yield a homogeneous amorphous solid that we hereafter call xerogel. In the case of the Mn, the xerogel showed traces of crystallized Mn_2O_3 within the amorphous material. The amount of the crystallized Mn_2O_3 phase, whose diffraction peaks correspond to γ-Mn_2O_3, depended on the drying kinetics. In order to avoid its formation, the most appropriate procedure was to dry the solutions at 85°C under vacuum in a rotating evaporator. Throughout the drying process, the homogeneity of the gelatinous precipitate is maintained and its viscosity increased. By stopping the drying at 90°C before completion, a viscous solution that can be deposited by spin coating (1000 rpm) onto stainless steel substrate is obtained. This allows the subsequent synthesis of $LiMn_2O_4$ thick films using the heat treatments to be described.

Results and Discussion

(I) Synthesis of Mn Spinels and Their Study

We first investigated the role of the starting materials (acetates vs nitrates) and ambient atmosphere (oxygen vs argon) on the

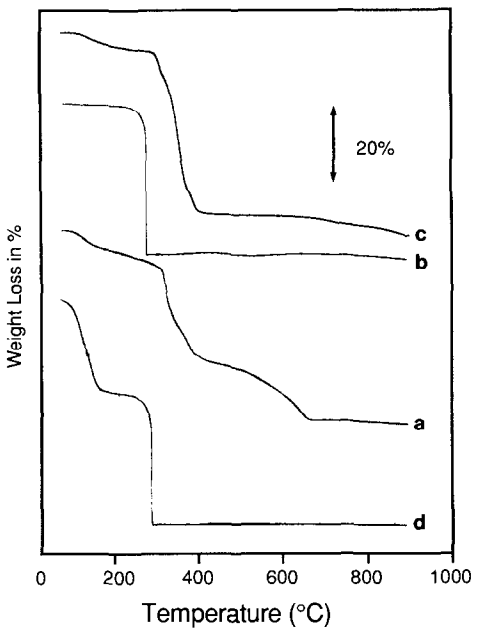

FIG. 1. Thermal analysis for Mn and Li coprecipitated phase in various ambients (a) coprecipitated acetates in argon, (b) coprecipitated acetates in oxygen, (c) coprecipitated nitrates in argon, and (d) a mixture of commercial LiOH and $Mn(OAc)_2 \cdot 4H_2O$ powders. The heating rate was 10°C/min.

synthesis of the $Li_xMn_2O_4$ phases by means of X-ray diffraction, infrared spectroscopy, thermogravimetric analysis (TGA) and differential thermogravimetry analysis (DTA) measurements.

(*a*) *Characterization of the materials.* Figure 1 demonstrates the difference in reactivity between acetate and nitrate xerogels for the case of Li/Mn = 1/2 (i.e., $LiMn_2O_4$). When the nitrates are used as precursors, the weight loss of the precipitate heated at a rate of 10°C/min in oxygen occurs in a few steps, including the formation of $LiNO_3$ and γ-Mn_2O_3, and it is not completed until temperatures greater than 600°C are reached (Fig. 1a). In contrast, with the acetate precipitate under similar heating conditions, the reaction is complete at 250°C (Fig. 1b) after a very exothermic decomposition of the acetate group occurs as shown in Fig. 2a. This decomposition is so violent that even for small amounts of sample used in the thermoanalysis experiments (~5 mg), the actual temperature is raised to 400°C at this stage of the thermal treatment. This explains the vertical decomposition obtained in the TGA apparatus (Fig. 1b). The infrared spectrum of the acetate precipitate dried at 150°C (Fig. 3a) does not show the presence of vibration modes associated with NH_3 or NH_4^+ groups, suggesting that these groups (introduced in the form of NH_4OH in the starting aqueous solution) have been completely removed during the drying step at 150°C. A TGA study of a manganese acetate precipitate (without Li) dried at 150°C has led to the composition $Mn(OAc)_{1.5}(OH)_{0.5}$, indicating, in addition to the loss of NH_4OH, the loss of water and of acetate

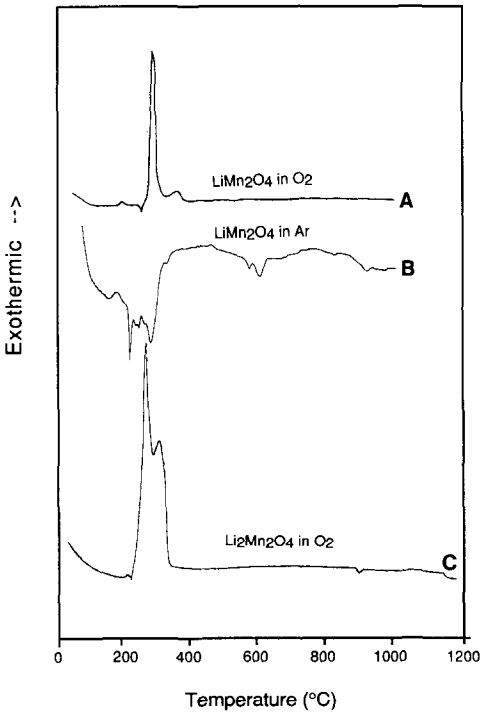

FIG. 2. Differential thermal analysis of (A) coprecipitated acetates in oxygen, (B) coprecipitated acetates in argon, and (C) a coprecipitate of nominal composition "$Li_2Mn_2O_4$" in oxygen. The heating rate was 10°C/min.

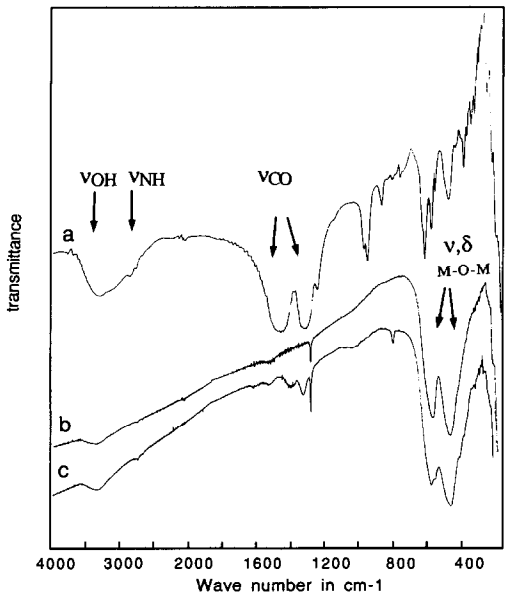

FIG. 3. Infrared spectrum of (a) acetate precipitate of nominal composition $LiMn_2O_4$ heat-treated at 150°C, (b) acetate precipitate of nominal composition $LiMn_2O_4$ heat-treated at 400°C, and (c) acetate precipitate of nominal composition $Li_2Mn_2O_4$ heat-treated at 400°C.

groups during the drying process at 150°C. Since the gelatinous precipitate is mostly due to the presence of manganese hydroxide it appears that drying results in the formation of some manganese acetate. An amorphous polymeric material is a consequence of the mixing of acetates and hydroxides as manganese ligands. Finally, a mixture of lithium hydroxide and manganese acetate powder (Fig. 1d) yields a similar behavior above 150°C as an acetate precipitate, although the completion of the reaction requires longer heating times. Thus, from the above findings the acetate precipitates can be considered as homogeneous mixtures of LiOH and $Mn(OAc)_{1.5}(OH)_{0.5}$ and their weight loss (Fig. 1b) could be accounted for by the following reaction:

$$LiMn_2(OAc)_3(OH)_2 + 15/2\ O_2 \rightarrow LiMn_2O_4 + 11H_2O + 6CO_2.$$

When the same TGA experiments are performed for the acetate precipitate in an argon ambient, we note a smoother exothermic decomposition (Figs. 1c, 2b) with an identical weight loss until a temperature of 600°C is reached. The resulting material was found to contain well-crystallized MnO, as determined by X-ray powder diffraction, and Li_2CO_3 as determined by infrared spectroscopy. Thus, the decomposition reaction could be written as

$$LiMn_2(OAc)_3(OH)_2 \rightarrow 1/2\ Li_2CO_3 + 2\ MnO + \cdots$$

It is only for temperatures greater than 600°C that Li_2CO_3 reacted with MnO to form the spinel $LiMn_2O_4$.

The thermal reactivity of the acetate xerogels was also found to be very dependant on the Li/Mn ratio denoted as r in the following. The most exothermic reaction happens for a mixture with $r = 0.5$ (i.e., $LiMn_2O_4$). This may be explained by the melting of the acetate mixture just before the decomposition as shown by the onset of an endothermic peak observed at 200°C in Fig. 2a. This melting initiates the very exothermic decomposition reaction that is immediately followed by a smaller exothermic peak at 350°C which may relate to the final reaction of the impurity γ-Mn_2O_3 phase with the remaining Li_2CO_3 to give the spinel structure. For Li/Mn ratios of 0 or 1, no liquid phase was observed and no melting was found in the DTA (Fig. 2c). The decomposition is then less violent and occurs in two steps. Depending on the Li concentration, the following results are obtained:

For $r = 0$, γ-Mn_2O_3 transforms to α-Mn_2O_3 above 400°C. For $0 < r < 0.5$, the materials obtained at 450°C are a mixture of the spinel structure $LiMn_2O_4$ and of the α-Mn_2O_3 phase. For $r = 0.5$, which yields a more reactive mixture, Mn_2O_3 is only observed as traces within a poorly crystallized $LiMn_2O_4$ phase at 250°C, as determined by X-ray analysis. At higher temperatures

(300°C), the Bragg peaks corresponding to Mn_2O_3 disappear and only diffraction peaks corresponding to the $LiMn_2O_4$ phase with $a = 8.23$ Å (as reported in the literature (*17*)) remain, indicating that this phase can be obtained at temperatures as low as 300°C.

For $0.5 < r < 1$, the $LiMn_2O_4$ spinel structure is mainly obtained without any change in the lattice parameters with increasing amounts of Li in the starting materials. During the first steps of the decomposition, Mn_2O_3, which transforms to $LiMn_2O_4$ upon heating for 12 hr at 300°C is observed. At higher temperatures (>400°C), an orange phase (Li_2MnO_3), as determined by X-ray analysis, is obtained at the surface of the powders. In addition, infrared spectroscopy on an acetate precipitate of nominal composition $Li_2Mn_2O_4$ heat-treated at temperatures above 400°C (Fig. 3c) shows the presence of carbonate groups that are not observed on an acetate precipitate of nominal composition $LiMn_2O_4$ heated at similar temperatures (Fig. 3b). Thus, the decomposition of the xerogel as a function of temperature with a Li/Mn = 1 ratio ($r = 1$), can then be written as

$$Li_2Mn_2(OAc)_3(OH)_2 \xrightarrow{250°C} Li_2CO_3 + \gamma\text{-}Mn_2O_3 + \cdots \text{volatile products}$$

then

$$\longrightarrow 1/2\ Li_2CO_3 + LiMn_2O_4 + \cdots \text{volatile products}$$

$$\xrightarrow{T>400°C} 2/3\ Li_2MnO_3 + 2/3\ LiMn_2O_4 + \cdots \text{volatile products}$$

It is obvious from the previous experiments that the "$Li_2Mn_2O_4$" phase (of potential interest for rocking-chair batteries) is not stable compared to the Li_2CO_3, $LiMn_2O_4$, and $Li_2Mn_2O_3$ phases when the samples are annealed in air. This is consistent with the observation that chemically prepared $Li_2Mn_2O_4$ decomposed at 300°C when heated in an oxygen ambient (*13*). In contrast, we have shown that in a nonoxidizing ambient (argon), this phase does not decompose until temperatures greater than 500°C are reached. We studied the effect of annealing at 400°C for 3 hr for several Li/transition-metal ratios (or r values), in various low oxygen pressures ($P(O_2) = 4$, 2, 0.5, 0.1% in argon). Independent of the r values or of the partial pressure of oxygen, the resulting materials were always multiphase with $LiMn_2O_4$ as the main phase and either cubic MnO or the orange phase Li_2MnO_3 as secondary phases. We previously showed that the first product of decomposition of an acetate precipitate heated in an argon ambient is Li_2CO_3, which is stable with respect to other Mn–O phases until $T > 500$°C. We believe that it is Li_2CO_3 which prevents the formation of the $Li_2Mn_2O_4$ phase even though this phase was reported to be stable in argon until 500°C. We thus concluded that the direct synthesis of $Li_2Mn_2O_4$ from acetates is impossible, independent of the ambient used. This result shows a discrepancy with the work of S. Bach *et al.* (*12*) in which they claim to obtain the $Li_2Mn_2O_4$ phase upon heating the mixture at temperatures above 930°C. However, the X-ray diffraction patterns published by these authors (Fig. 3b, Ref. (*12*)) unambiguously prove that the $Li_2Mn_2O_4$ phase that they obtain at this temperature is not the spinel structure but the layered phase $LiMnO_2$.

From this study we conclude that operating in argon or having a Li/M ratio greater than 0.5 yields the formation of Li_2CO_3, which shifts the formation of $LiMn_2O_4$ toward higher temperatures. The lower synthesis temperature (300°C) was achieved upon annealing in air an acetate precipitate having $r = 0.5$. To determine how the annealing temperature of the precipitate affects the morphology and crystallinity of the resulting $LiMn_2O_4$ powders, a systematic study was undertaken. Precipitates having $r = 0.5$ were separately annealed for 24 hr at temperatures of 300, 400,

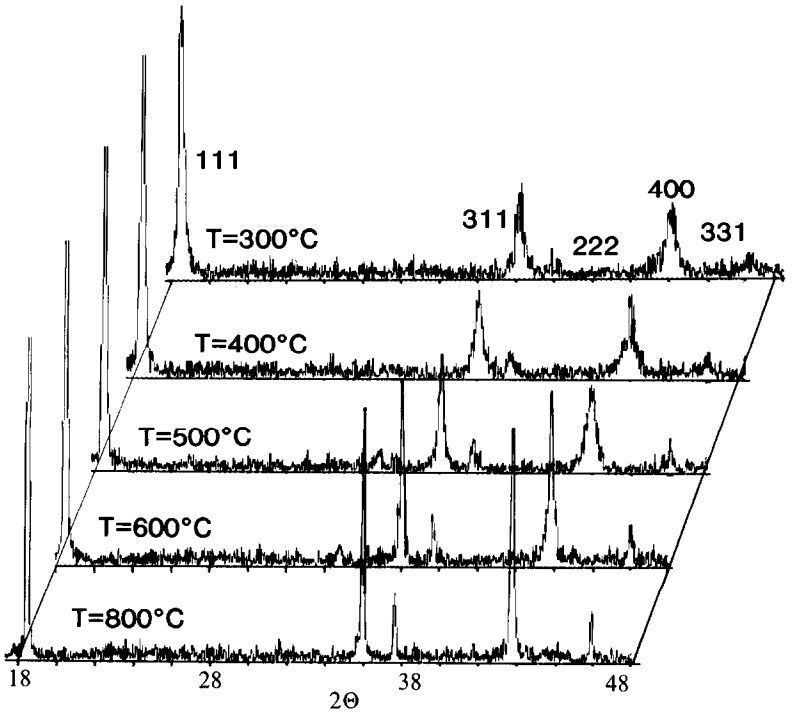

FIG. 4. X-ray powder diffraction patterns for $LiMn_2O_4$ as a function of the synthesis temperatures; 300, 400, 500, 600, and 800°C. The Miller indices are given for each Bragg peak.

500, 600, and 800°C, cooled, ground, pressed into pellets, and reannealed for another 24 hr at similar temperatures. The X-ray diffractograms of these powders are shown in Fig. 4. Note that the spinel phase forms at T = 300°C and that with increasing annealing temperatures the position of the Bragg diffraction peaks remain unchanged in contrast to their width, which sharpens continuously with increasing T. It is also interesting to note, for samples prepared at low temperatures, that the widths of the Bragg peaks increase noticeably with increasing scattering angle, suggesting the presence of residual strain. In Fig. 5 we plotted $B(2\Theta) * \cos^2(\Theta)$ (where $B(2\Theta)$ is the width of the Bragg peak at half of its maximum intensity) as a function of $\sin^2(\Theta)$ for the samples made at 800, 600, and 500°C. It has been demonstrated that such a plot should be linear if the strain and domain-size broadening add as a Gaussian convolution, and if so, the intercept with the origin gives the structural coherence length (domain-size) while the slope provides the residual strain (*14*). Our data indicate that the intercept remains more or less of the same order within the accuracy of our measurements (strongly limited by the small number of peaks (three) that are used), suggesting no drastic changes in the domain size between compounds prepared at 500 and 800°C. However, we note a drastic change in the slope of the lines, namely a decrease in the slope with increasing temperature indicating a much larger residual strain in the samples prepared at 500°C than at 800°C. We conclude that residual strain rather than particle size is governing the changes in the width of the Bragg peaks observed as a function of temperature.

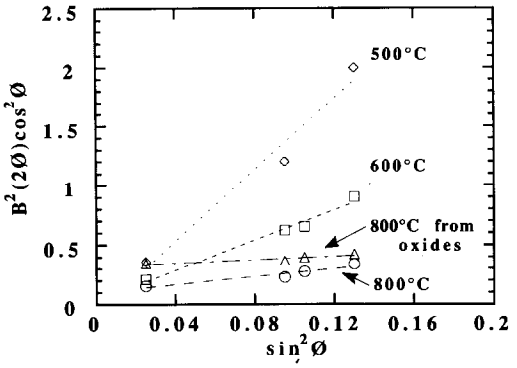

FIG. 5. The linewidth at half intensity $B(2\Theta)$ of the Bragg peaks multiplied by $\cos^2(\Theta)$ is plotted as a function of $\sin^2(\Theta)$ for the $LiMn_2O_4$ samples prepared at 400, 500, 600, and 800°C from acetates and at 800°C from oxides.

The residual strain may arise from defects such as composition inhomogeneities, cationic or anionic nonstoichiometry, grain boundaries, or polymorphism (MnO_2 is well known for this (*15*)) that vanish with increasing temperature as one usually expects.

(*b*) *Electron microscopy.* The $LiMn_2O_4$ powders prepared by heating the acetate precipitates at temperatures of 300, 400, 500, 600, and 800°C were investigated by scanning electron microscopy (SEM). Figures 6a and 6b show only the most characteristic micrographs. The powders contain crystallites exhibiting cubic crystal facets at temperatures as low as 300°C, with grain size ranging from ≤ 0.03 to 0.1 μm (Fig. 6a). At higher temperatures, growth kinetics are favored and larger grains are observed as the annealing temperature is increased so that for a sample heated at 800°C the grain size ranges from 0.1 to 3 μm (Fig. 6b). This factor of 10 in the particle size observed between samples prepared at 300 and 800°C by no means can account for the large change in the width of the Bragg peak observed by X-rays between the two samples. Both X-ray and SEM studies show that by simply varying the thermal processing (time, temperature, and the heating steps sequence) $LiMn_2O_4$ powders with a wide variety of defect and microcrystallite morphologies could be obtained. Next, we show the effect of processing conditions on electrochemical properties.

(*c*) *Cycling behavior.* The resulting $LiMn_2O_4$ powders prepared at 300, 400, 500, 600, and 800°C were studied for their Li intercalation properties using swagelock test cells (*16*) assembled in a helium drybox. About 20 mg of $LiMn_2O_4$ powders were mixed with 10% black carbon, pressed into a pellet, and used as the positive electrode. Lithium metal was used as the negative electrode. Both electrodes were separated by a porous glass filter soaked in an electrolyte made by dissolving 1 *M* LiClO4 + 1 *M* 12-crown-4 ether in propylene carbonate. The assembled cells containing $LiMn_2O_4$ powders synthesized at various temperatures were automatically tested and equivalently charged and discharged at constant current rate while the potential was monitored as a function of time. The composition is automatically calculated from the current, the mass of the cathode, and the elapsed time. The cycling data for these cells over the range of potential 4.5–3.5 V (corresponding to the first Li intercalation plateau ($LiMn_2O_4 \leftrightarrow \lambda$-$MnO_2$)) and over the potential range 3.5–2.2 V (corresponding to the second Li intercalation plateau ($LiMn_2O_4 \leftrightarrow Li_2Mn_2O_4$)) are shown in Figs. 7a and 7b, respectively. A general remark is that the shape of the charge and discharge curves for each potential range are characteristic of the manganese-oxide spinel structure (*9, 17, 18*) even for the sample annealed at 300°C (*11*). Note that when considering the first intercalation plateau at 4.0 V for the 300°C sample that the capacity is lower than expected and the polarization is larger. This can be related to the presence of unreacted Mn_2O_3 or most likely to defects in the structure. The 400°C sample shows larger capacity and less polarization. Upon further increasing of the syn-

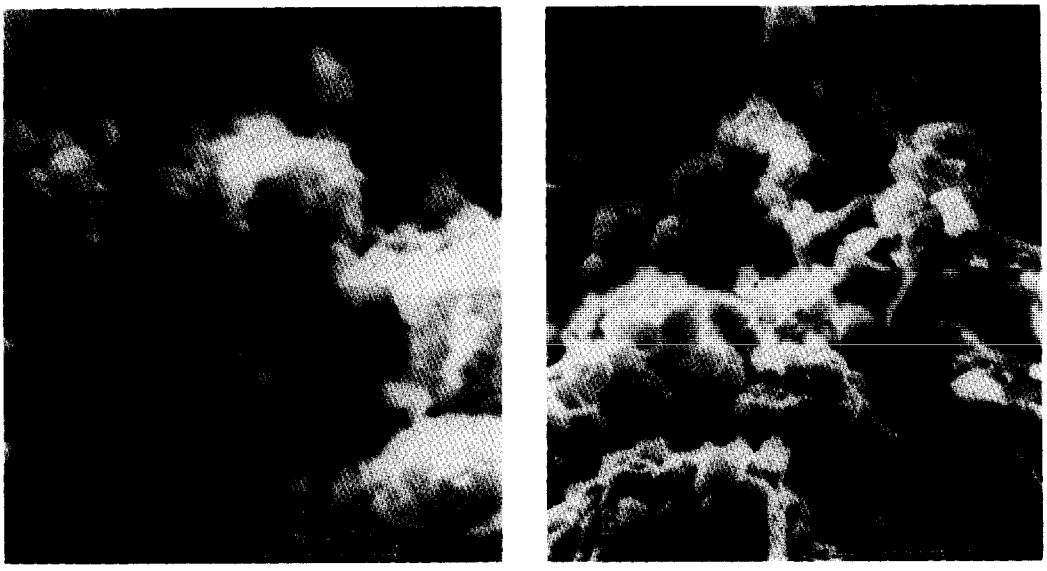

FIG. 6. Scanning electron micrographs for $LiMn_2O_4$ samples heat-treated at (a) 300°C and (b) 800°C.

thesis temperature of the positive electrode, the capacity of the cells increases from 64 to 78% when a cathode made at 400°C is replaced by a cathode made at 800°C. In contrast, the reverse trend is observed when the cells are cycled around the second Li intercalation plateau (3.5–2.2 V). Indeed, the largest capacity and the best cycling behavior is observed when $LiMn_2O_4$ was synthesized at 300°C.

We have previously shown that a cell using $LiMn_2O_4$ as the positive electrode shows poor reversibility over the same range of voltage (3.5–2.2 V) and this behavior was ascribed to the large volume change (12%) between the $LiMn_2O_4$ and the $Li_2Mn_2O_4$ phases. The fact that our samples made at 300°C show very good reversibility with respect to Li intercalation at this voltage range may suggest (i) that by increasing the amount of defects it becomes easier for the material to accomodate the 12% volume change associated with the intercalation process or, more likely, (ii) that by using the low-temperature synthesis one may favor the formation of a small amount of amorphous or badly crystallized phase at the grain boundary (nondetectable by X-ray analysis) that could intercalate Li reversibly over this range of potential. We should recall that cells using a positive electrode of unknown crystal structure, made by heating a mixture of LiOH + MnO_2 (EMD) at 400°C, have also shown good cyclability over this range of potential. The presence of this unknown phase will not affect the capacity of the cells when cycled between 3.5 and 2.2 V but should affect the capacity of the 4.5–3.2 V range, consistent with our experimental data. The typical cycling behavior of a cell using $LiMn_2O_4$ synthesized at 400°C as the positive electrode between 4.5 and 2 V is shown in Fig. 8a. The charge and discharge curves are similar to those previously reported for cells using a $LiMn_2O_4$ phase prepared at temperatures of

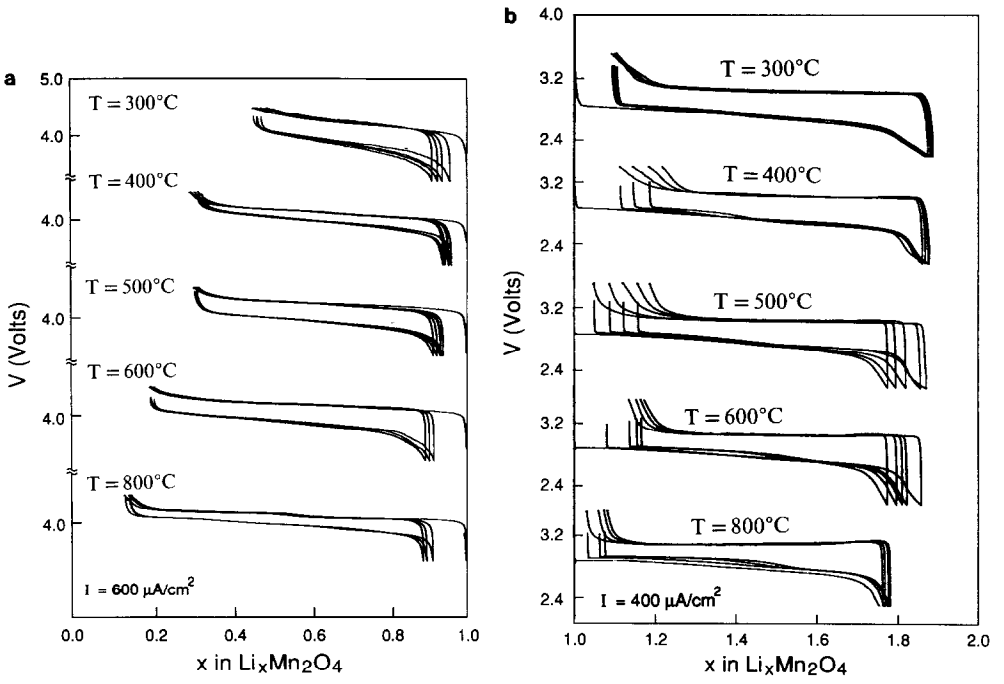

FIG. 7. Cycling data at a current rate of 600 $\mu A/cm^2$ between 4.5 and 3.5 V (**a**) and between 3.5 and 2.2 V (**b**) for cells using $LiMn_2O_4$ powders annealed at 300, 400, 500, 600, and 800°C as positive electrodes.

800°C as the positive electrode, indicating that the impurity phase that may be responsible for the loss of capacity at 4 V has vanished upon heating the sample to 400°C.

Finally, another advantage of the solution synthesis technique over solid state reactions is that thick films could be made, and in Fig. 8b we report the cycling behavior of one of these films, 10 μm thick, that has been made by dipping a stainless steel substrate into a viscous acetate aqueous solution, dried in air, and then heated in air for 16 hr at 600°C. The cycling data obtained using these films as the positive electrode are similar to those measured for bulk. These results indicate that this material can be shaped in various forms without affecting its electrochemical behavior.

(II) Synthesis of the Layered $LiMO_2$ Phases (M = Ni, Co)

We have applied a similar solution technique to the synthesis of other Li containing materials such as $LiMO_2$ (M = Ni, Co) of potential interest for the development of rocking-chair batteries. For Co, using the acetates as the precursors, the $LiCoO_2$ phase is obtained starting from 300°C after 12 hr. For Ni, independent of the starting composition, the processing temperature, and the time of treatment, we always obtained Li_2CO_3 and NiO as the resulting phases. Dahn *et al.* (*19*) succeeded in forming the Li_xNiO_2 at 650°C but never formed lithium carbonate. We may conclude that the decomposition of acetates into carbon-

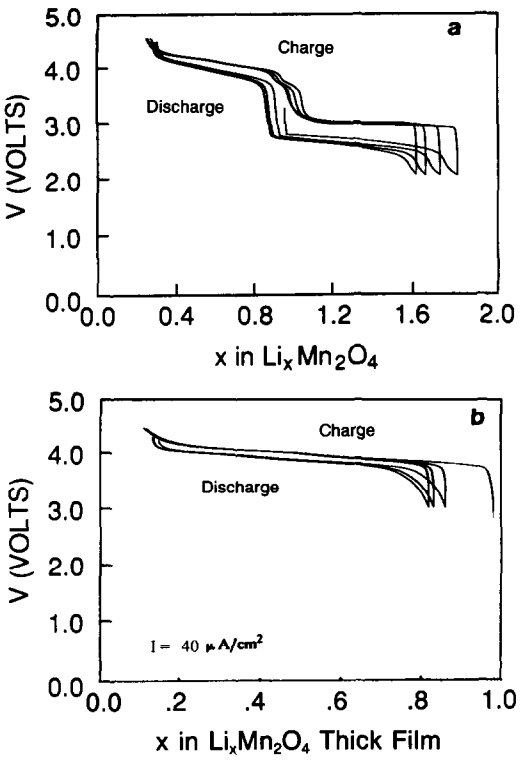

FIG. 8. Typical cycling behavior over the potential range 4.5–2.2 V at a current rate of 800 μA/cm^2 for cells using $LiMn_2O_4$ synthesized at 400°C as the positive electrode is shown in a. In b the cycling behavior between 4.5 and 3.5 V at a current rate of 40 μA/cm^2 is shown for a cell using a 10 μm $LiMn_2O_4$ thick film prepared by dipping (see text).

ates leads to the formation of lithium carbonate, which is stable toward reaction with nickel oxide. Indeed, starting from nitrates, the $LiNiO_2$ phase can be obtained but without any real decrease of the reaction temperature as compared to the solid state synthesis already described (*19*). This is related to the poor reactivity of the nitrates as already demonstrated in the case of manganese (*11*). In all of these phases, the 3*d* transition metal has an oxidation state equal or greater than 3. Such a high oxidation state for the 3*d* metal is possible within an oxide framework structure. Therefore, the difficulty of achieving this oxidation state increases with 3*d* metals further to the right in the periodic table (for instance it is extremely difficult to prepare compounds with Cu^{+3}). This observation may explain the better reactivity of cobalt and manganese acetates compared to nickel, in forming a phase in which the 3*d* metal has to be +3. The use of oxygen pressure should favor the stability of Ni^{+3} and thereby the stability of the layered phase $LiNiO_2$. We are presently investigating the annealing of acetate nitrate precipitates under oxygen pressure.

(*III*) *Synthesis of Na Containing Phases*

Finally, we further show the versatility of the acetate precursor route by synthesis studies of the $Na_xMn_2O_4$ system. Acetates and NaOH instead of LiOH was used to prepare the composition with $x = 1$ (a systematic study of the composition effect will be described elsewhere). The X-ray pattern of a sample of nominal composition $NaMn_2O_4$, heat-treated at various temperatures, is shown in Fig. 9. The xerogel is amorphous below 200°C but at $T = 200$°C exhibits the same exothermic reaction as in the Li case. It yields a poorly crystallized material whose X-ray pattern, given in Fig. 9a, cannot be attributed to any known phases. Its corresponding electrochemical behavior in the case of sodium intercalation is shown in Fig. 10a. A smooth and continuous decrease of the voltage is observed during the intercalation. Note also that it is impossible to remove more than 0.25 Na per Mn from the starting composition. This yields a formula $Na_{0.25}MnO_2$. This phase transforms upon heat-treatment at higher temperature (850°C) to the structure of the $Na_{0.44}MnO_2$ phase described by J. P. Parent *et al.* (*20*) as shown by X-ray diffraction studies in Fig. 9c. This structure exhibits interesting electrochemical behavior characterized by many phase transitions during the intercalation of sodium

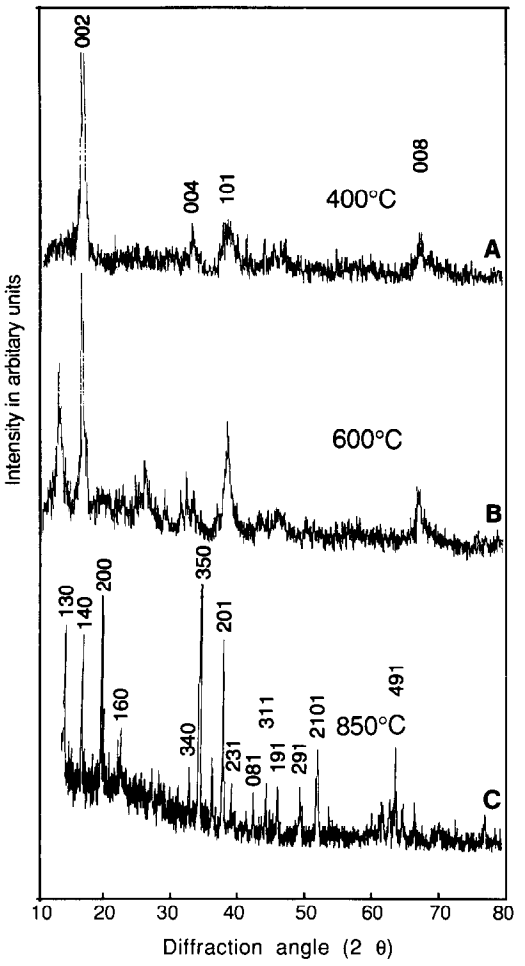

FIG. 9. X-ray powder diffraction pattern of materials of nominal composition $NaMn_2O_4$ heat-treated at (A) 400°C, (B) 600°C, and (C) 850°C.

as shown in Fig. 10b. The nature of these transitions will be described elsewhere.

Conclusion

The synthesis of oxides from aqueous solutions offers a low-cost, versatile low-temperature method for producing powders with small grain sizes that may lead to improved electrochemical properties, namely better rechargeability. We have shown that the use of transition-metal acetates carefully hydrolyzed by raising the pH of the solution with mixtures of lithium and ammonium hydroxides yields homogeneous precipitates and gels. However, a phase separation occurs upon heat treatment between lithium carbonate and the transition-metal oxide. The powders remain very reactive in the case of Mn and Co and yield submicron particles of intercalation compounds. Nickel remains unreactive. The control of the concentration and the aging of the solution yields gels having a viscosity which is suitable for thick-film deposition using spin

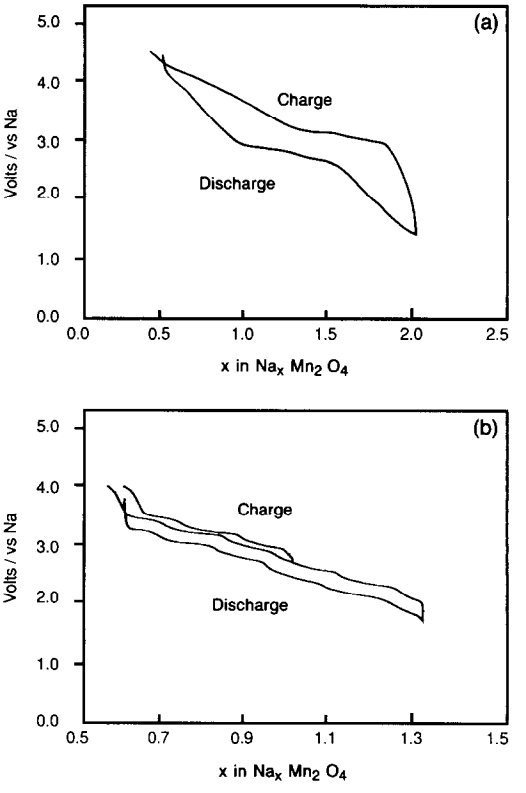

FIG. 10. The cycling behavior of cells using the material of nominal composition $NaMn_2O_4$ heat-treated at 400 and 850°C as positive electrodes is shown in a and b, respectively.

coating, as demonstrated in the case of lithium manganese oxide. This would offer a low-cost process for covering large areas of electrode material for film cells.

Acknowledgments

We thank D. Guyomard, P. F. Miceli, and J. H. Wernick for helpful comments and technical discussions.

References

1. D. W. Murphy, F. J. DiSalvo, J. N. Carides, and J. V. Waszczak, *Mater. Res. Bull.* **13,** 1395 (1978).
2. K. Mizushima, P. C. Jones, P. J. Wiseman, and J. B. Goodenough, *Mater. Res. Bull.* **15,** 783 (1980).
3. J. J. Auborn and Y. L. Barbario, *J. Electrochem. Soc.* **134,** 638 (1987).
4. J. M. Tarascon, *J. Electrochem. Soc.* **132,** 2089 (1985).
5. K. Tozawa, "Rechargeable Battery Conference, Tokyo, March 3–5, 1990."
6. J. R. Dahn, U. von Sacken, and R. Fong, Presented at the Primary and Secondary Lithium Batteries Symposium of the 178th Electrochemical Society Meeting, Seattle, October 14–19, 1990.
7. "Sony's Lithium Manganese Rechargeable Battery (AA size)," JEC Press Inc., (February, 1988).
8. Moli Energy's New Product Data Sheet, *JEC Battery Newslett.* **6,** 15 (1988).
9. J. M. Tarascon, E. Wang, F. Shokoohi, W. R. McKinnon, and S. Colson, submitted for publication.
10. T. Katsurai, *Bull. Chem. Soc. Jpn.* **18,** 277 (1943) and other references quoted in *Gmelin Handbuch* **56**(C1), 374 (1973).
11. E. J. Cuy *J. Phys. Chem.* **25,** 415 (1920–1921) and other more recent references in *Gmelin Handbuch,* **56**(C1), 422 (1973).
12. S. Bach, M. Henry, N. Baffier, and J. Livage, *Solid State Chem.* **88,** 325 (1990).
13. J. M. Tarascon and D. Guyomard, submitted for publication.
14. H. P. Klug and L. E. Alexander, "X-Ray Diffraction Procedures For Polycrystalline And Amorphous Materials," Wiley, New York (1954).
15. M. Ripert, J. Pannetier, and Y. Chabre, "Solid State Ionics Symposium, Mater. Res. Soc. Meeting Boston, November 26, December 1, 1990." [Abstract L7.4]
16. J. M. Tarascon, F. J. Disalvo, D. W. Murphy, G. W. Hull, and J. V. Waszczak, *J. Solid State Chem.* **54,** 204 (1984).
17. M. M. Thackeray, W. I. F. David, P. G. Bruce, and J. B. Goodenough, *Mater. Res. Bull.* **18,** 461 (1983).
18. M. M. Thackeray, P. J. Johnson, L. A. de Picciotto, P. G. Bruce, and J. B. Goodenough, *Mater. Res. Bull.* **19,** 179 (1984).
19. J. R. Dahn, U. von Sacken, and C. A. Michal, *Solid State Ionics* **44,** 87 (1990).
20. J. P. Parent, R. Olazcuaga, M. Devalette, C. Fouassier, and P. Hagenmuller. *J. Solid State Chem.* **3,** 1 (1971).